

The crystallization of $Gd_2O_3 - Al_2O_3$ glasses

TOETSU SHISHIDO

*The Oarai Branch, The Research Institute for Iron, Steel and Other Metals,
Tohoku University, Oarai, Ibaraki-ken, 311-13 Japan*

Glasses of $Gd_2O_3 \cdot x Al_2O_3$ compositions where x represents 5/3, 4 and 6, were prepared using a rapid quenching apparatus and a laser beam. The crystallization process of the glasses was studied by means of differential thermal analysis (DTA), X-ray diffraction analysis and electron microscopy. The crystallizations of $Gd_2O_3 \cdot 5/3 Al_2O_3$, $Gd_2O_3 \cdot 4 Al_2O_3$ and $Gd_2O_3 \cdot 6 Al_2O_3$ are complex and exhibit one, two and three exothermic peaks in DTA measurement with increasing Al_2O_3 concentration, respectively. The crystallization process of $Gd_2O_3 \cdot 5/3 Al_2O_3$ glass involved the direct formation of the gadolinium aluminium garnet, $3Gd_2O_3 \cdot 5Al_2O_3$ (GdAG), which is not obtained by the ordinary solid phase reaction. After crystallization of $Gd_2O_3 \cdot 4 Al_2O_3$ and $Gd_2O_3 \cdot 6 Al_2O_3$ glass, both phases become a mixture of $Gd_2O_3 \cdot Al_2O_3$ (perovskite type) and $\alpha-Al_2O_3$.

1. Introduction

Synthesis of oxide glasses by rapid quenching has been studied by many researchers [1-3]. The present authors have previously studied the glass formation of high melting-point oxide compounds with a lanthanide oxide (Ln_2O_3) as the main component. In the $Ln_2O_3 - Al_2O_3$ system ($Ln = La$ to Lu , and Y), the composition range giving a glassy state was determined. The crystallization process of the $Ln_2O_3 \cdot 6 Al_2O_3$ glass was classified into three groups depending on the different Ln elements [2].

In the present study, the glassy state of $Gd_2O_3 \cdot x Al_2O_3$ ($x = 5/3, 4$ and 6) was prepared. The melt of a eutectic composition has a strong tendency for glass formation by rapid quenching because of the high viscosity [4]. Similar results have been obtained at our laboratory [6]. For this reason, the compositions of $x = 5/3, 4$ and 6 in the vicinity of the eutectic composition were selected. In addition, Gd was chosen from among the lanthanides because its atomic number and atomic radius rank in the middle of the lanthanides. The crystallization process was examined in relation to the phase diagram and the Al_2O_3 concentration of the glass.

2. Experimental details

99.9% pure powder Gd_2O_3 and 99.995% pure powder $\alpha-Al_2O_3$ were mixed in 3:5, 1:4 and 1:6 molar ratios. The mixture was cold-pressed into pellets 5 mm diameter and 1 mm thick under a pressure at 4000 kg cm^{-2} . The pellets were then sintered at 1000°C for 5 h in air, and crushed into pieces of 1 to 2 mm diameter. These pieces were melted and quenched at a cooling rate of $\sim 8 \times 10^7^\circ \text{C sec}^{-1}$ in a piston-anvil type quenching apparatus using a laser beam [5], so that the glassy state could be achieved. The crystallization process of the glasses was studied by DTA and X-ray diffraction as reported previously [6]. A diffraction pattern and a light-field image by a JEM-200A transmission electron microscope operating at an acceleration voltage of 200 kV were taken to study the details of the crystallization process.

3. Results and discussion

3.1. Glasses in the $Gd_2O_3 - Al_2O_3$ system

The compositions and phase diagram [7] of $Gd_2O_3 - Al_2O_3$ are shown in Fig. 1. In the phase diagram, the eutectic point is at about 78 mol% Al_2O_3 . In the case of the composition with

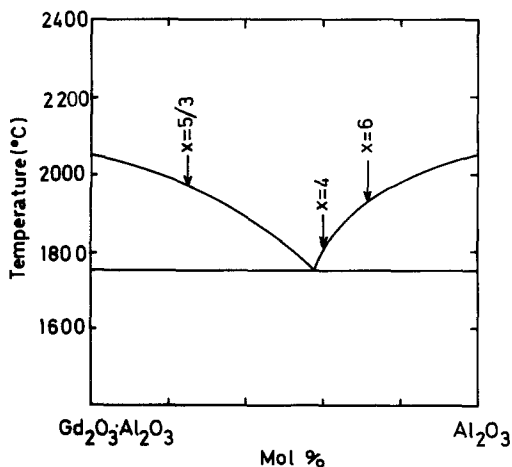


Figure 1 Compositions of $Gd_2O_3 \cdot xAl_2O_3$ glasses in the phase diagram of $Gd_2O_3 \cdot Al_2O_3 - Al_2O_3$.

$x = 5/3$, the Al_2O_3 concentration is lower than the eutectic composition, while for the cases of $x = 4$ and $x = 6$, the Al_2O_3 concentration is higher than the eutectic composition. In transmission electron microscopy of the glass samples, the electron diffraction pattern showed a typical halo and the light-field image showed no crystalline phase.

DTA measurements were made for the glass samples of the three different Al_2O_3 concentrations. The DTA curves are shown in Fig. 2. With increasing Al_2O_3 concentration, the number of exothermic peaks increases, i.e. one, two and three peaks for $x = 5/3$, 4 and 6, respectively. None of the compositions showed exothermic or endothermic peaks during cooling. From the DTA results, the crystallization temperature and the crystallization heat were examined and the values shown in Table I. It is shown that the crystallization initiation temperature, i.e. the temperature where the first exothermic peak appears in DTA, is closely related with the liquidus tempera-

TABLE I Thermal properties of $Gd_2O_3 \cdot xAl_2O_3$ glasses

x	Crystallization initiation temperature T_{c1} ($^{\circ}C$)	Crystallization heat ΔH_c ($kcal\ mol^{-1}$)	Liquidus temperature in phase diagram T_l ($^{\circ}C$)
$\frac{5}{3}$	937	3.70	1950
4	910 1007	1.33 0.71	1790
6	922 1101 1248	1.74 0.57 0.97	1920

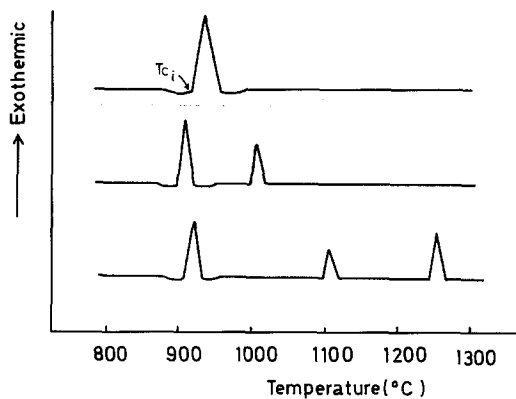


Figure 2 DTA curves of $Gd_2O_3 \cdot xAl_2O_3$ glass.

ture in the phase diagram. An increase in the liquidus temperature results in an increase in the crystallization initiation temperature. The heats of crystallization obtained were 2.04 to 3.70 $kcal\ mol^{-1}$.

3.1.1. Crystallization process of $Gd_2O_3 \cdot 5/3Al_2O_3$ glass

Fig. 3a to c shows the results of electron microscopy for the composition with $x = 5/3$ (garnet composition) in the crystallization process. Fig. 3a is for the unheated glass, while Fig. 3b shows the sample heated to $950^{\circ}C$ after the appearance of one exothermic peak. The electron diffraction pattern exhibits spots due to the crystalline phase and the light-field image indicates precipitated crystal grains. The diffraction spots are evidently caused by the gadolinium aluminium garnet, $3Gd_2O_3 \cdot 5Al_2O_3$ (GdAG), phase. Fig. 3c shows the sample heated to $1300^{\circ}C$. Both the electron diffraction pattern and the light-field image indicate crystal growth of the GdAG phase.

The garnet phase obtained by solid phase reaction in the $Ln_2O_3 - Al_2O_3$ system is reported for Ln from Tb, next to Gd in atomic number, to Lu and Y [8, 9]. However, GdAG is not obtained by solid phase reaction; it is synthesized by the flux crystal growth method using $PbO - PbF_2$ as the flux [10, 11]. In the present study, it was shown that the GdAG phase can be prepared by synthesizing the garnet composition glass and then heating it at elevated temperatures. Fig. 4 shows X-ray powder diffraction patterns for $x = 5/3$ in the course of heating. With increasing temperature, the peak due to the garnet phase becomes more sharp. Crystal structure analysis was made for the sample heated at $1300^{\circ}C$ for 1 h using

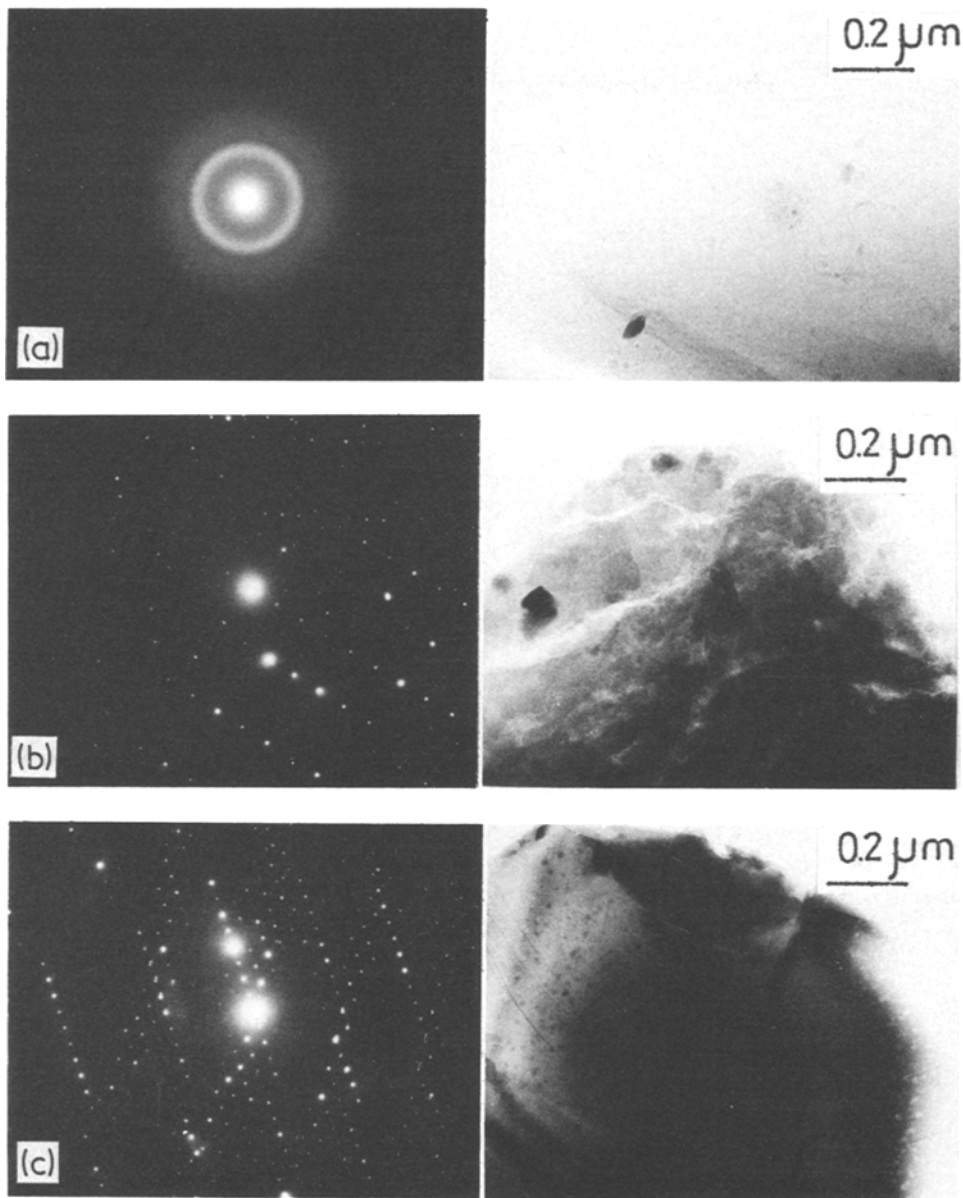


Figure 3 Electron micrographs of the crystallization process of $Gd_2O_3 \cdot 5/3Al_2O_3$. (a) Without heat-treatment, (b) heated to $950^\circ C$, (c) heated to $1300^\circ C$, (d) heated to $1500^\circ C$.

X-ray powder diffraction measurements. The GdAG phase formed was of a cubic system with lattice constant $a = 12.111 \pm 0.005 \text{ \AA}$. The value was close to $a = 12.106 \pm 0.005 \text{ \AA}$ [10] and $a = 12.110 \text{ \AA}$ [11] for the GdAG phases synthesized by the flux crystal growth method. The values of d_{obs} and d_{calc} of the GdAG phase are shown in Table II. The values of d_{calc} were calculated using the value of $a = 12.111 \text{ \AA}$.

3.1.2. Crystallization process of $Gd_2O_3 \cdot 4Al_2O_3$ glass

Fig. 5a to c shows the results of electron microscopy for $x = 4$ in the crystallization process. Fig. 5a shows the glass before heating, and Fig. 5b the sample after heating above the first exothermic peak (heated to $950^\circ C$). The electron diffraction pattern is similar to that for the glass, but the light-field image shows very little difference from

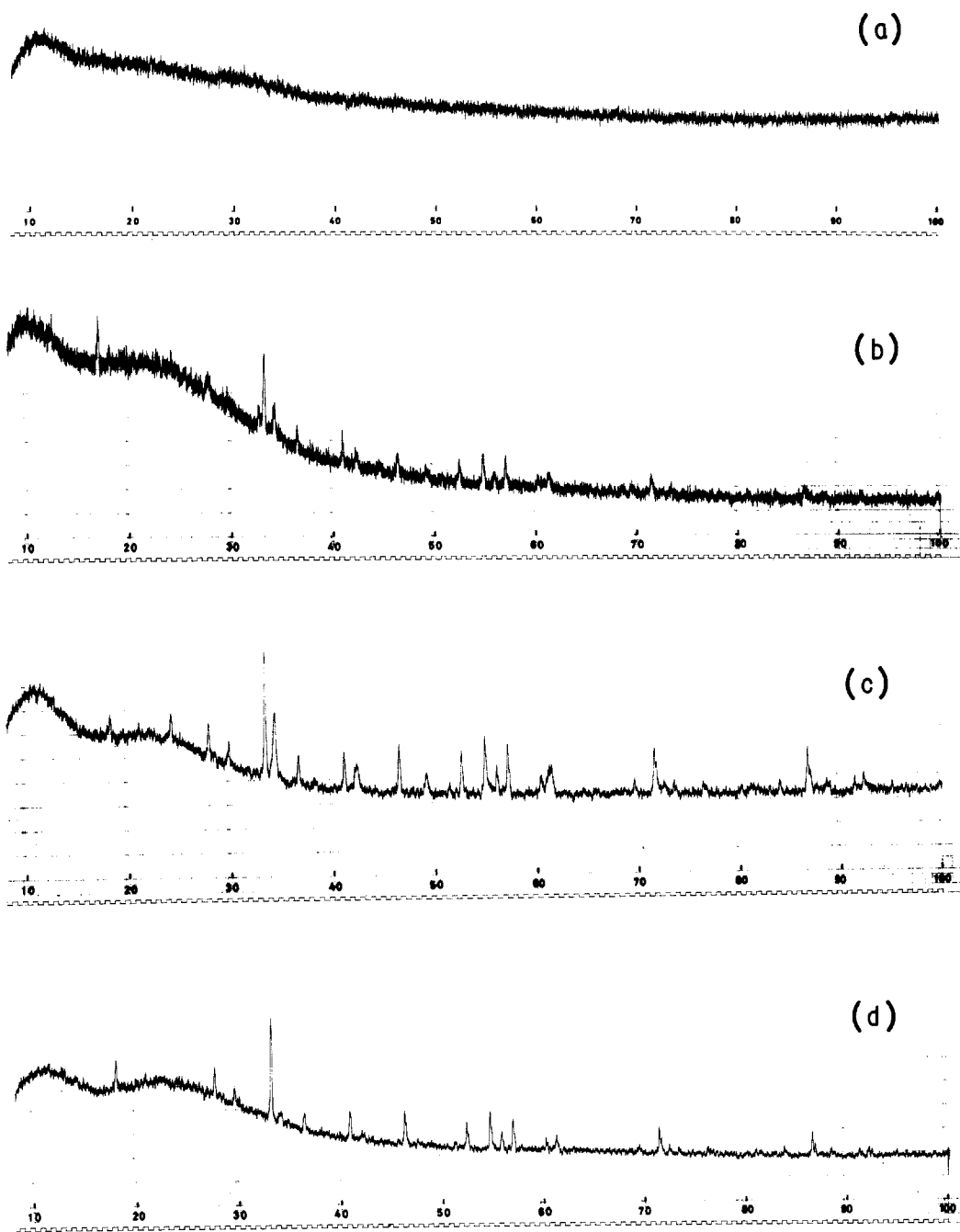


Figure 4 Variation of the X-ray powder diffraction pattern with heat-treatment of the $\text{Gd}_2\text{O}_3 \cdot 5/3\text{Al}_2\text{O}_3$ glass. (a) Without heat-treatment, (b) 950°C , 1 h heated in air, (c) 1300°C , 1 h heated in air, (d) 1500°C , 1 h heated in air.

TABLE II Values of d_{obs} and d_{calc} of the GdAG phase obtained in heating $\text{Gd}_2\text{O}_3 \cdot \frac{5}{3} \text{Al}_2\text{O}_3$ glass

hkl	d_{calc} (Å)	d_{obs} (Å)	I_{obs}
2 1 1	4.944	4.950	m
2 2 0	4.282	4.284	w
3 2 1	3.237	3.240	w
4 0 0	3.028	3.029	m
4 2 0	2.708	2.711	vs
4 2 2	2.472	2.470	s
5 2 1	2.211	2.213	m
4 4 0	2.141	2.144	vw
6 1 1, 5 3 2	1.965	1.966	m
4 4 4	1.748	1.750	m
6 4 0	1.679	1.679	m
7 2 1, 6 3 3	1.648	1.649	vw
6 4 2	1.618	1.617	m
7 3 2, 6 5 1	1.538	1.541	vw
8 0 0	1.514	1.516	w
8 4 0	1.354	1.352	w
8 4 2	1.321	1.324	m
9 2 1, 7 6 1	1.306	1.307	vw
6 6 4	1.291	1.290	vw
10 3 1	1.155	1.155	w
10 4 0, 8 6 4	1.124	1.124	m
11 2 1, 10 5 1	1.079	1.080	w
8 8 0	1.070	1.069	w
12 4 4	0.9129	0.9127	w
12 6 0, 10 8 4	0.9027	0.9024	w
14 4 0, 12 8 2	0.8318	0.8318	w
14 4 2, 12 6 6	0.8240	0.8240	w

that in the glassy state. This seems to suggest a stage of nucleation. Fig. 5c shows the sample after the second exothermic peak (heated to 1300°C). Both the electron diffraction pattern and the light-field image indicate growth of the crystalline phase. Diffraction rings are due to the GdAlO_3 and $\alpha\text{-Al}_2\text{O}_3$ phases.

3.1.3. Crystallization process of $\text{Gd}_2\text{O}_3\text{-}6\text{Al}_2\text{O}_3$ glass

Fig. 6a to d show the results of electron microscopy. Fig. 6a shows the glass before heating, and Fig. 6b the sample after the first exothermic peak (heated to 950°C). The electron diffraction pattern is similar to that for the glass, but spots due to precipitated fine grains are slightly visible. The light-field image differs little from that for the glass. Nuclei formation is indicated. Fig. 6c shows the sample after the second exothermic peak (heated to 1250°C). The electron diffraction pattern and the light-field image are of precipitated ultra-fine crystal grains of uniform size. The diffraction ring is due to the GdAlO_3 phase. The

sample after the third exothermic peak (heated to 1300°C) is shown in Fig. 6d. The electron diffraction pattern and the light-field image indicate the growth of the crystalline phase. The diffraction rings show a phase mixture of the GdAlO_3 and $\alpha\text{-Al}_2\text{O}_3$ phase.

4. Conclusions

The glassy state of $\text{Gd}_2\text{O}_3 \cdot x\text{Al}_2\text{O}_3$ ($x = 5/3, 4$ and 6) was prepared with a rapid quenching apparatus using the laser beam. The crystallization process of these glasses are summarized in Table III. In heating the glass, the crystallization process is influenced by the Al_2O_3 concentration (x). The higher crystallization initiation temperature is obtained for the composition with a higher liquidus temperature in the phase diagram. The crystallization process of the $\text{Gd}_2\text{O}_3 \cdot 5/3\text{Al}_2\text{O}_3$ glass with an Al_2O_3 concentration lower than the eutectic composition ($\text{Gd}_2\text{O}_3\text{-}78\text{ mol}\% \text{Al}_2\text{O}_3$) involves the direct formation of gadolinium aluminium garnet, $3\text{Gd}_2\text{O}_3 \cdot 5\text{Al}_2\text{O}_3$ (GdAG), without any intermediate metastable phase. Such a gadolinium aluminium garnet phase is not obtained by the ordinary solid phase reaction. The crystallization processes of $\text{Gd}_2\text{O}_3 \cdot 4\text{Al}_2\text{O}_3$ and $\text{Gd}_2\text{O}_3 \cdot 6\text{Al}_2\text{O}_3$ glasses with Al_2O_3 concentrations higher than the eutectic composition are complex and exhibit two and three exothermic peaks by DTA, respectively. The phase after the final crystallization at 1300°C is a mixture of the perovskite and $\alpha\text{-Al}_2\text{O}_3$ phases in both compositions, as shown in Table III.

Acknowledgement

The author is deeply indebted to Professor S. Yajima and Dr K. Okamura for helpful discussions on the present study.

References

1. P. T. SARJEANT and R. ROY, *J. Amer. Ceram. Soc.* **50** (1967) 500.
2. S. YAJIMA, K. OKAMURA and T. SHISHIDO, *Chem. Letters* (1973) 1327.
3. J. P. COUTURES, J. COUTURES, G. BENEZECH and E. ANTIC, "Proceedings of the 12th Rare Earth Research Conference", Vol. II, C. E. Lundin (ed.) (Denver Research Institute, 1976) p. 626.
4. H. RAWSON, "Inorganic Glass Forming Systems" (Academic Press, London and New York, 1967).
5. S. YAJIMA, K. OKAMURA and T. SHISHIDO, *Chem. Letters* (1974) 1531.

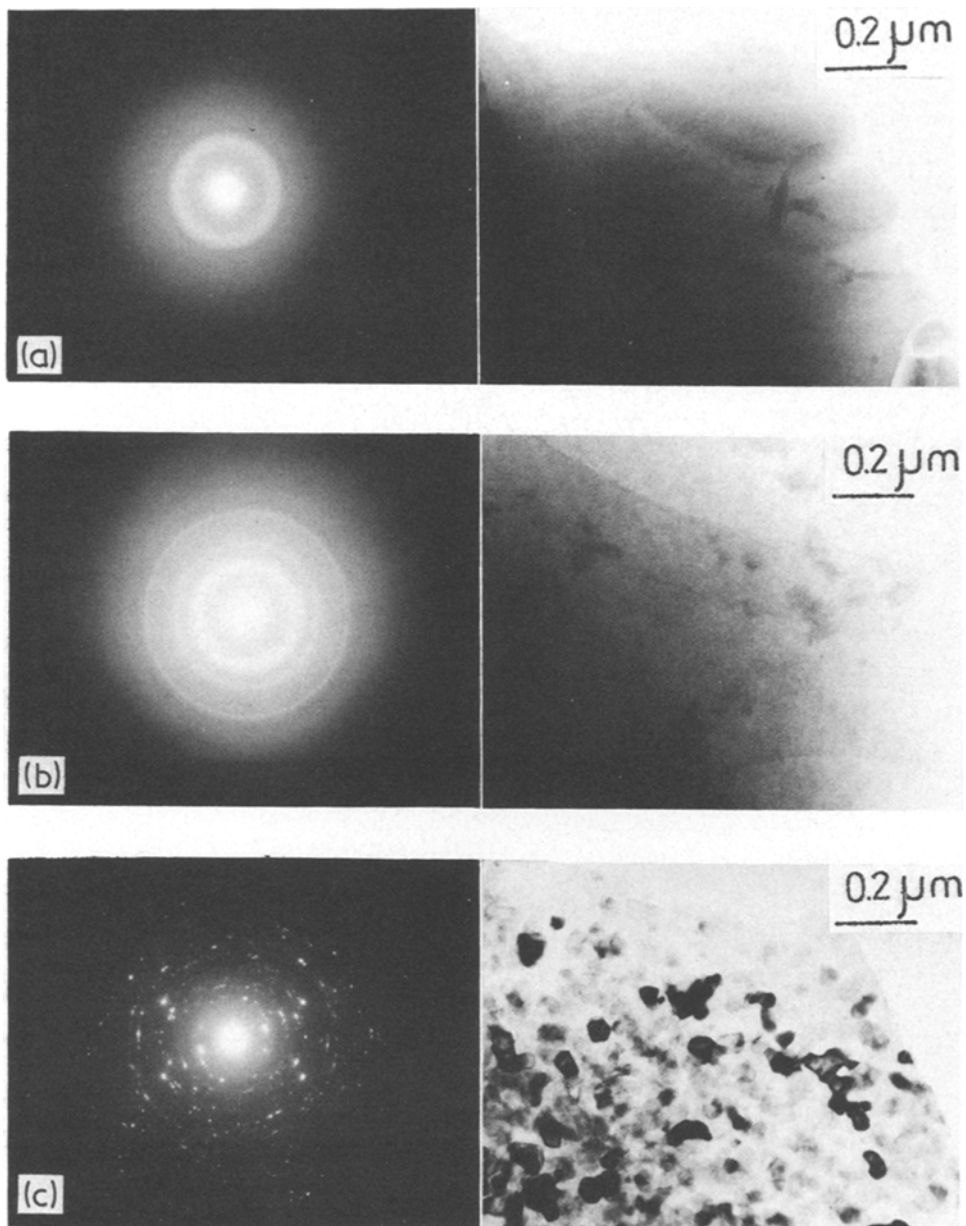


Figure 5 Electron microscope observation in the crystallization process of $Gd_2O_3 \cdot 4Al_2O_3$ glass. (a) Without heat-treatment, (b) heated to $925^\circ C$, (c) heated to $1300^\circ C$.

TABLE III Crystallization process of $Gd_2O_3 \cdot xAl_2O_3$ glasses

$x = \frac{5}{3}$	Glassy phase	————	Garnet phase
$x = 4$	Glassy phase	————	Nuclei formation ———— Perovskite phase + $\alpha-Al_2O_3$ phase
$x = 6$	Glassy phase	————	Nuclei formation ———— Perovskite phase ———— Perovskite phase + $\alpha-Al_2O_3$ phase

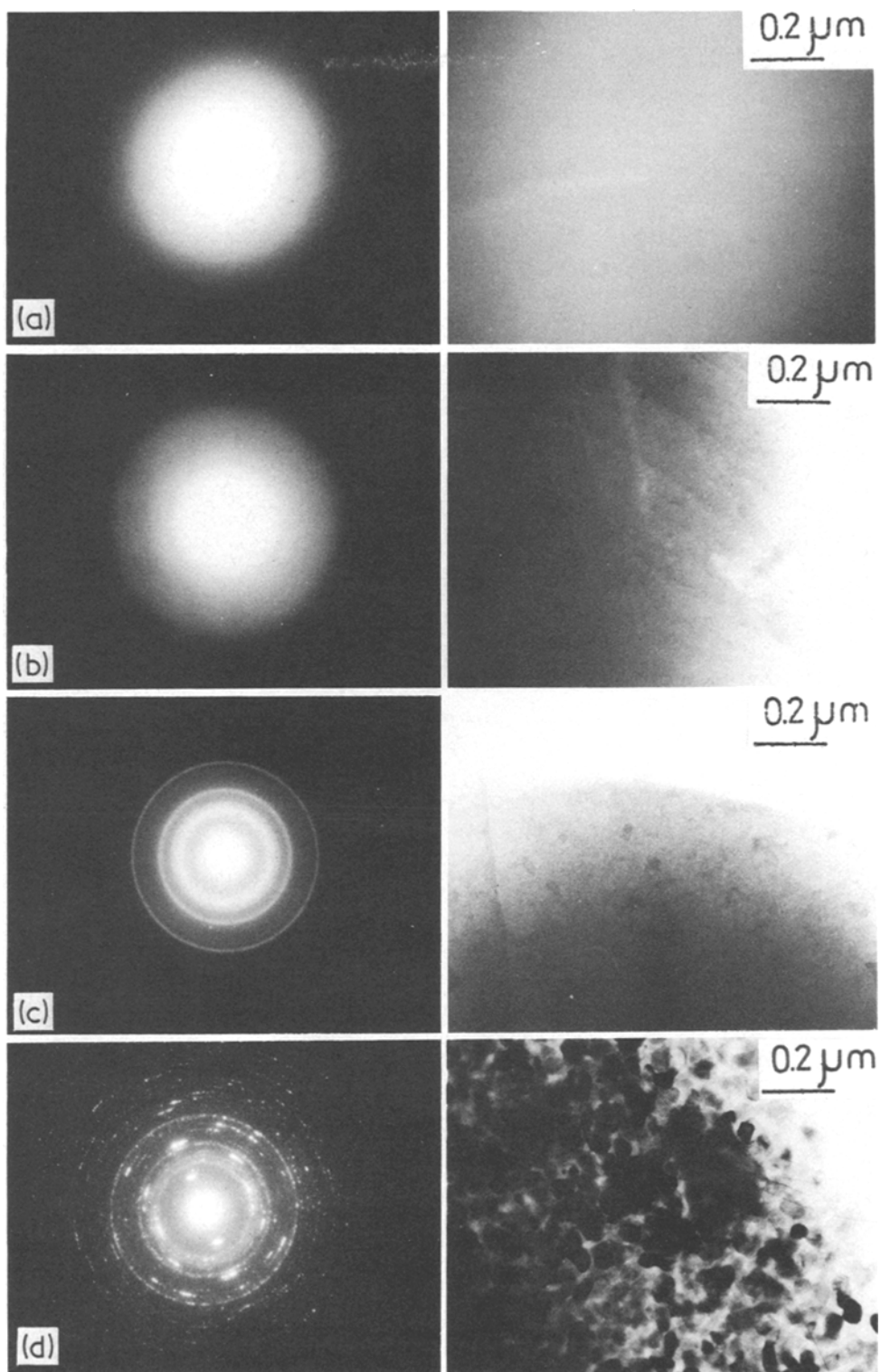


Figure 6 Electron micrographs of the crystallization process of $Gd_2O_3 \cdot 6Al_2O_3$ glass. (a) Without heat-treatment, (b) heated to $950^\circ C$, (c) heated to $1125^\circ C$, (d) heated to $1300^\circ C$.

6. T. SHISHIDO, K. OKAMURA and S. YAJIMA, *J. Mater. Sci.* **13** (1978) 1006.
7. P. P. BUBNIKOV, V. I. KUSHAKOVSKII and V. S. BELEVANTSEV, *Dokl. Akad. Nauk SSR* **165** (1965) 1077.
8. S. J. SCHNEIDER, R. S. ROTH and J. L. WARING, *J. Res. Nat. Bur. Stand.* **65A** (1961) 364.
9. T. NOGUCHI and M. MIZUNO, *Kogyo Kagaku Zasshi* **70** (1967) 839.
10. T. MANABE and K. EGASHIRA, *Mat. Res. Bull.* **6** (1971) 1167.
11. L. G. VAN UITERT, W. H. GRODKIEWICZ and E. F. DEARVORN, *J. Amer. Ceram. Soc.* **48** (1965) 105.

Received 14 March and accepted 6 July 1978.